Journal of Fluorescence (2019) 29:1065–1077
https://doi.org/10.1007/s10895-019-02425-w

FLUORESCENCE NEWS ARTICLE

A Novel Switch on Optical Probe for Selective Sensing of Zn (II) Ion in Acetonitrile Medium: Spectroscopic and Computational Studies

Mahantesh Budri[1] · Geeta Chimmalagi[1] · Ganesh Naik[1] · Shivaraj Patil[2] · Kalagouda Gudasi[1] · Sanjeev Inamdar[2]

Received: 29 May 2019 / Accepted: 29 July 2019 / Published online: 11 August 2019

Keywords Optical probe · Zn(II) ion · ESIPT/ICT process · Bioimaging · Theoretical investigations

Introduction

An emerging research area in present days for the monitoring of trace metal ions is to design and synthesis of an efficient, economical and targeted metal ion/ions responsive sensors [1–5]. Chemosensors are the conjugated organic molecules, which upon interacting with analyte produce detectable optical responses [6]. Out of several available optical sensors, fluorescent chemosensors are getting considerable attention due to their intrinsic sensitivity, upfront application in real-time monitoring with their quick responses [7, 8]. In recent years, 'Turn On' fluorescence sensors are attracting much attention for monitoring the trace level metal ions in the environmental as well as biological processes [9, 10].

The development of optical chemosensors is mainly focusing on d block elements because of their essentiality in biological and environmental processes [11]. Any analytical technique or detection technique which are able to detect or quantify the essential or toxic metal ions are of great interest in the diagnosis of environmental and biological issues. Among transition metal ions, being second most abundant metal ion in human body after iron, zinc regulates many important physiological and pathological processes [8, 12]. Even though zinc is believed to be present in coordinated form in enzymes and proteins, few studies reported its free ionic form in biological system [13]. Zinc is considered to be relatively nontoxic in lower concentration whereas, it is toxic in high intakes [14, 15].

Even though many analytical techniques are reported in literature for the measurement of Zn^{2+} ion [16–19] but they suffer with one or the other disadvantages like huge capital investment, complicated procedures, low sensitivity, time consuming and also require skillful users. Therefore, for quick, accurate and simpler detections, a new analytical tool is much essential. The present research in the field suggests the colorimetric and fluorescent sensors but further understanding and improved accuracy is required for their on-field applications [8, 17].

The common requirements for the fluorescent chemosensors are the fluorophore and chelating unit. Generally, fluorophores are designed using either aromatic, polyaromatic units or heterocyclic moieties with conjugated double bond systems [20]. When conjugated organic molecules interact with the analyte, the optical properties of system changes which involves many chemical reactions and produce either change in color (colorimetric analysis) or fluorescence intensity (fluorescence method) [6]. The nitrogen of a Schiff base is generally known for its highest affinity for Zn(II) ion. Hence, our research for the construction of zinc chemosensor is mainly focussed on Schiff base [9, 10]. Literature study reveals that, there are only few chemesensors reported till date containing di-*tert*- butyl group as substituents. This functional group is well known to increase the ICT (Intramolecular Charge Transfer) character when attached to an aromatic ring with electron withdrawing groups [21].

In our continuous effort to synthesize novel optical sensors for zinc ion, in this study we have synthesized ESIPT (Excited State Intramolecular Proton Transfer) and ICT (Inter/Intra

Highlights
- A novel sensor TBH was developed for the recognition of Zn(II) ion.
- The host exhibits significant optical response for Zn(II) ion.
- TBH is much selective for Zn(II) ion with lower detection limit.
- The practical usefulness of TBH for Zn(II) ion was tested in HeLa cells.
- The receptor could be easily recyclable using suitable reagent.

Electronic supplementary material The online version of this article (https://doi.org/10.1007/s10895-019-02425-w) contains supplementary material, which is available to authorized users.

✉ Kalagouda Gudasi
drkbgudasi@kud.ac.in

[1] Department of Chemistry, Karnatak University, Dharwad 580003, India

[2] Department of Physics, Karnatak University, Dharwad 580003, India

molecular charge transfer) process oriented fluorescent chemosensor; (*E*)-*N*′-(2-hydroxybenzylidene)-3, 5-di-*tert*-butyl-2-hydroxybenzohydrazide (**TBH**). The optical response towards different cations such as Li^+, Na^+, K^+ (MNO_3), Ca^{2+}, Mg^{2+}, Mn^{2+}, Ba^{2+}, Cu^{2+}, Co^{2+}, Ni^{2+}, Hg^{2+}, Pb^{2+}, Cd^{2+} ($M(NO_3)_2$) and Al^{3+} ($M(NO_3)_3$) were studied to check the selectivity of **TBH** for Zn(II) ion. Among these metal ions, **TBH** is found to be very much selective for Zn(II) ion with a lower detection limit as compared to our earlier work [22].

Experimental Section

Materials and Methods

All the chemicals and reagents used for experiments were of analytical and spectroscopic grade. The IR spectra were obtained on a PerkinElmer Spectrum Two FT-IR spectrometer in the 4000–550 cm^{-1} region. The ^{1}H-NMR spectra were recorded in DMSO-d_6 on Bruker 400 MHz spectrometer with tetramethylsilane (TMS) as the internal standard. Mass spectra were recorded on a Waters-XEVO TQS micro mass spectrometer and Shimadzu QP 2010S GC-Mass spectrometer. Electronic spectra were recorded using UV-Visible spectrophotometer (PerkinElmer Lambda 365) in 200–1100 nm range using acetonitrile as the solvent. The fluorescence spectra were measured on Fluoromax - 4 Spectrofluorometer (Horiba Scientific make). The elemental analyses (C, H, N) were carried out using a Thermoquest CHN analyzer. The conductivity of solutions was measured using ELICO CM 180 Conductivity meter.

Synthesis of (*E*)-*N*′-(2-hydroxybenzylidene) -3,5-di-*tert*-butyl-2-Hydroxybenzo Hydrazide (TBH)

An 3,5-di-*tert*-butyl-2-hydroxybenzohydrazide was synthesized as earlier reported by our research group [22]. Finally, **TBH** was synthesized by slow addition of a methanolic solution of salicylaldehyde (1 g; 8 mmol) to a methanolic solution of 3,5-di-*tert*-butyl-2-hydroxybenzohydrazide (2 g; 8 mmol) and stirred for 5 h. The yellow solid obtained was washed with methanol and dried in air.

Color: White, yield: 85%, m.p: 258–260 °C, Anal. Calcd for $C_{22}H_{28}N_2O_3$ (%): C, 71.71; H, 7.66; N, 7.60. Found (%): C, 70.90; H, 7.55; N, 7.58. IR (cm^{-1}): 3450 (O-H, broad), 3198 (N-H), 1624 (C=O), 1609 (C=N). ^{1}H-NMR (400 MHz, DMSO-d_6, ppm): 1.32 (9H, s, *tert*-Bu, C19H, C20H, C21H), 1.39 (9H, s, *tert*-Bu, C13H, C14H, C15H), 7.45 (1H, d, C16H, J = 2 Hz), 8.78 (1H, s, C7H), 7.74 (1H, d, C22H, J = 2 Hz), 11.08 (1H, s, N2H), 12.99 (1H, s, O3H), 12.15 (1H, s, O1-H), 7.61 (C1H, dd, J = 1.6 & 7.6 Hz), 7.32 (1H, ddd, C3H, J = 1.64 & J = 7.8 Hz), 6.96–6.92 (2H, m, C2H and C4H); ^{13}C-NMR (100 MHz, DMSO-d_6, ppm): 31.27 ($(CH_3)_3$), 34.20 ($(CH_3)_3$), 29.19 (C-$(CH_3)_3$), 34.70 (C-$(CH_3)_3$), 116.40 (C6), 157.45 (C7), 167.34 (C8), 136.54 (C11), 128.43 (C16), 139.73 (C17), 121.24 (C22), 110–140 (C1-C4, aromatic). EI-MS: m/z – 368 $[M]^+$.

Isolation of Zinc Complex

A acetonitrile solution of $Zn(NO_3)_2.6H_2O$ (0.38 g, 0.13 mmol) was added dropwise to acetonitrile solution of **TBH** (0.5 g, 0.13 mmol) and refluxed for 5 h. The

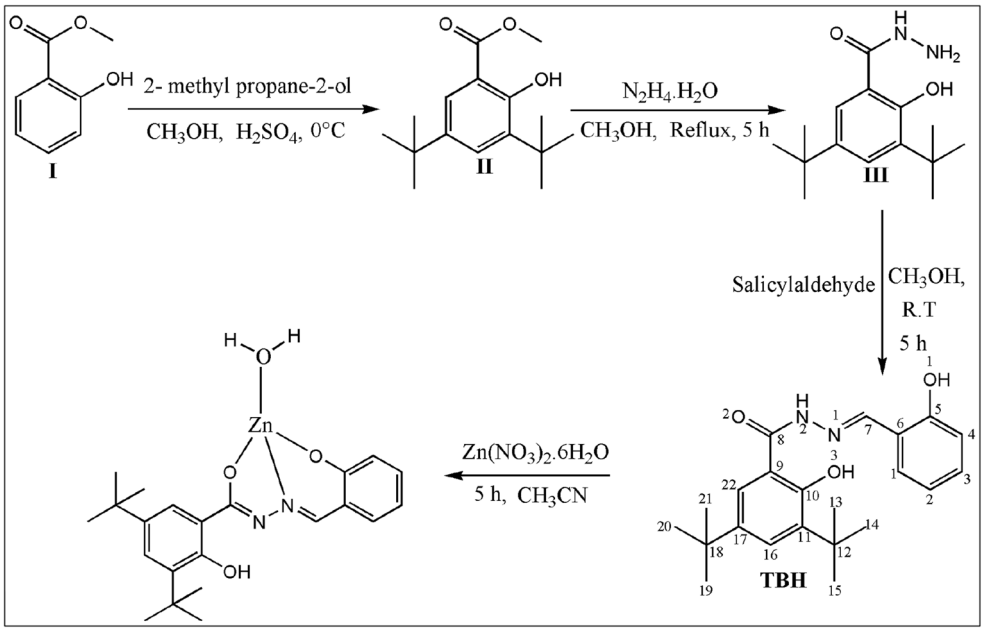

Scheme 1 Synthetic route for TBH and its coordinating behavior towards Zn^{2+}

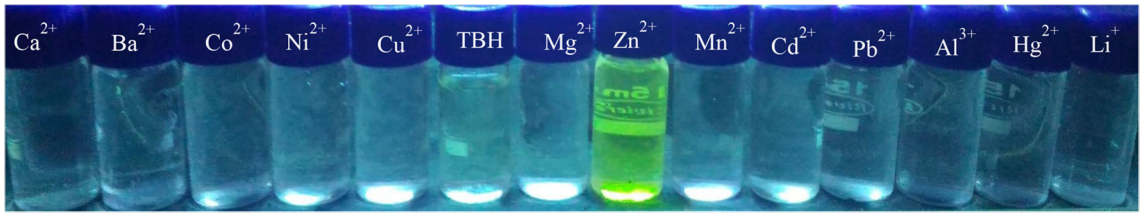

Fig. 1 Color change of receptor TBH (1×10^{-5} M soln. in CH_3CN) after the addition of 300 μL (1 equiv.) of respective cations (1×10^{-3} M soln.) in CH_3CN

yellow solid obtained was filtered and washed with cold methanol to get the desired product.

Color: Yellow, yield: 82%, Anal. calcd for $C_{22}H_{28}N_2O_4Zn$ (%): C, 58.75; H, 6.27; N, 6.23; Zn, 14.54. Found (%): C, 58.60; H, 6.25; N, 6.19; Zn, 14.40. IR (cm^{-1}): 3442 (O-H), 1601 (C=N), 1617 (C=N, new), 1246 (C-O). ^{1}H-NMR (400 MHz, DMSO-d_6, ppm): 1.30 (9H, s, *tert*-Bu, C19H, C20H, C21H), 1.42 (9H, s, *tert*-Bu, C13H, C14H, C15H), 8.57 (1H, s, C7H), 14.17 (1H, s, O3-H), 6.00–8.00 (Ar-6H), ESI-MS (m/z): 451 $[M + H]^+$. Molar conductance (Ω^{-1} cm^2 mol^{-1}): 4.55.

Theoretical Calculations

Gaussian 09 software was used for theoretical calculations [23] and input structures of **TBH** and its zinc complex were built by Gaussview-5.0. The optimized geometries were obtained by using the density functional theory and excited state energy calculations were performed employing time-dependent density functional theory. For both the methods, B3LYP correlation function was used. In the calculation, split valence basis set 6-311G (d) augmented with diffuse function and Los Alamos effective core potentials plus the Double Zeta (LanL2DZ) basis set [24] were applied.

Fluorescence Imaging Studies

HeLa cells cultured in DMEM were treated with 10 μM **TBH** for 30 min at 37 °C to check its fluorescence emission. The application of **TBH** for Zn(II) ion detection in HeLa cells was investigated by incubating 10 μM Zn(II) ion in DMEM for 30 min at 37 °C. After washing thrice with Phosphate buffer saline, HeLa cells emission was recorded using Zeiss LSM 710 confocal microscope (Leica).

Results and Discussion

The **TBH** and its zinc complex is synthesized as shown in Scheme 1.

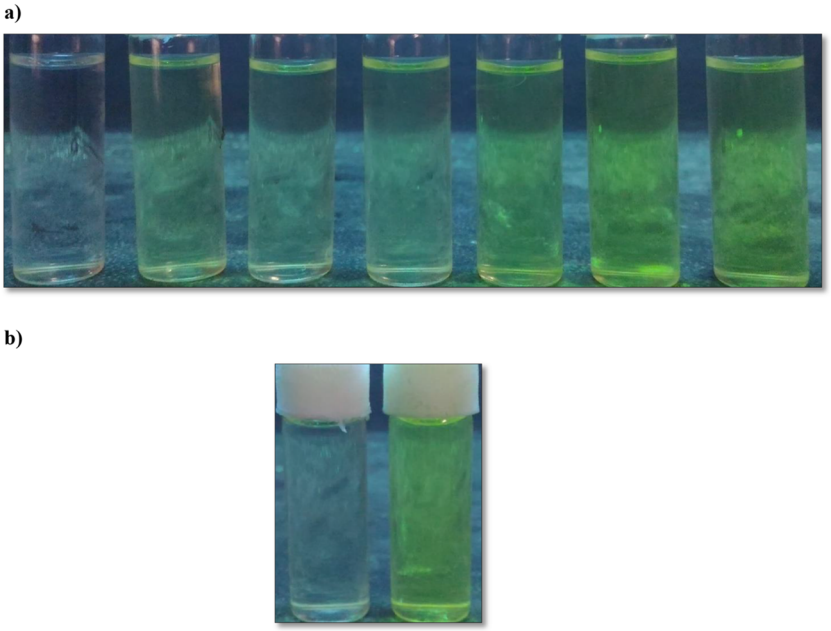

Fig. 2 **a** Change in the intensity of color of receptor TBH (1×10^{-5} M soln. in CH_3CN) after increasing addition of Zn^{2+} (50 to 300 μL, 1×10^{-3} M soln.) in CH_3CN. **b** Immediate color change of TBH (1×10^{-5} M soln. in CH_3CN) upon addition of Zinc ion (1×10^{-3} M soln. in CH_3CN)

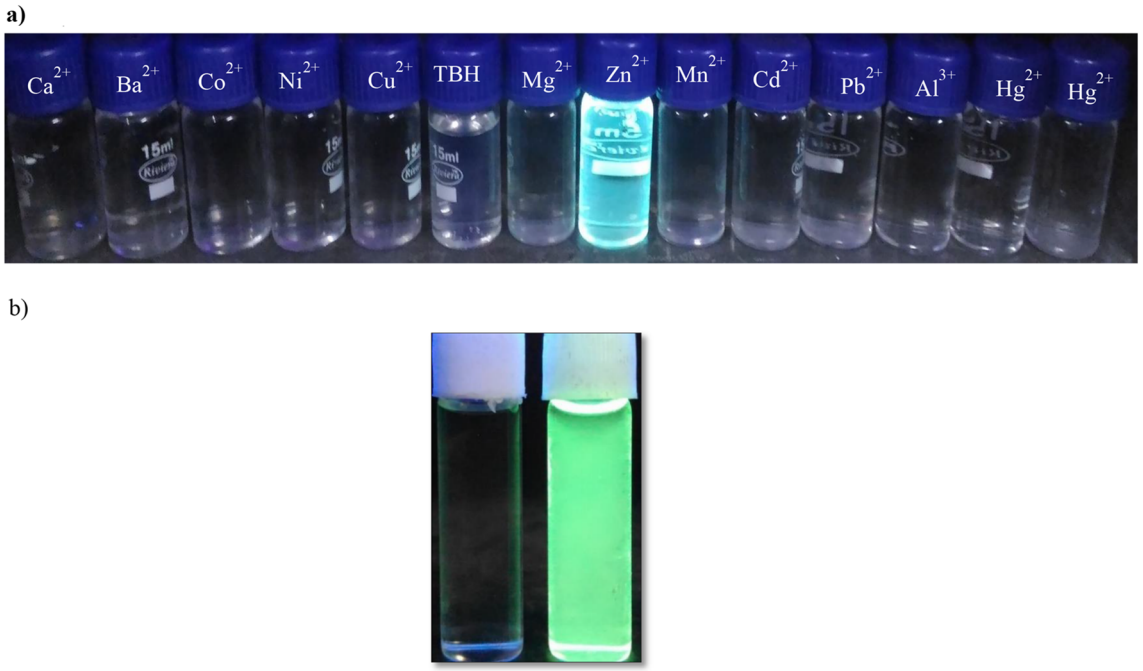

Fig. 3 **a** The photographs of the solution of TBH (1×10^{-5} M) in the presence of various metal ions (10 equiv.) under the UV light at 390 nm. **b** rapid color change of TBH (1×10^{-5} M) in the presence Zinc (II) ion (1×10^{-3} M soln. in CH_3CN)

A novel zinc selective 'turn on' fluorescent candidate is designed, synthesized and screened for bioimaging studies. The sensor is designed with the aim; to make it i) highly selective for Zn(II) ion ii) highly soluble in any common solvents iii) to enhance ICT character upon coordination and, iv) to block ESIPT and -C=N isomerization upon coordinating with zinc [9, 10]. The Zn(II) ion sensing ability of **TBH** is visible even by nacked eyes and it looks intense fluorescent under UV light (Figs. 1, 2, and 3).

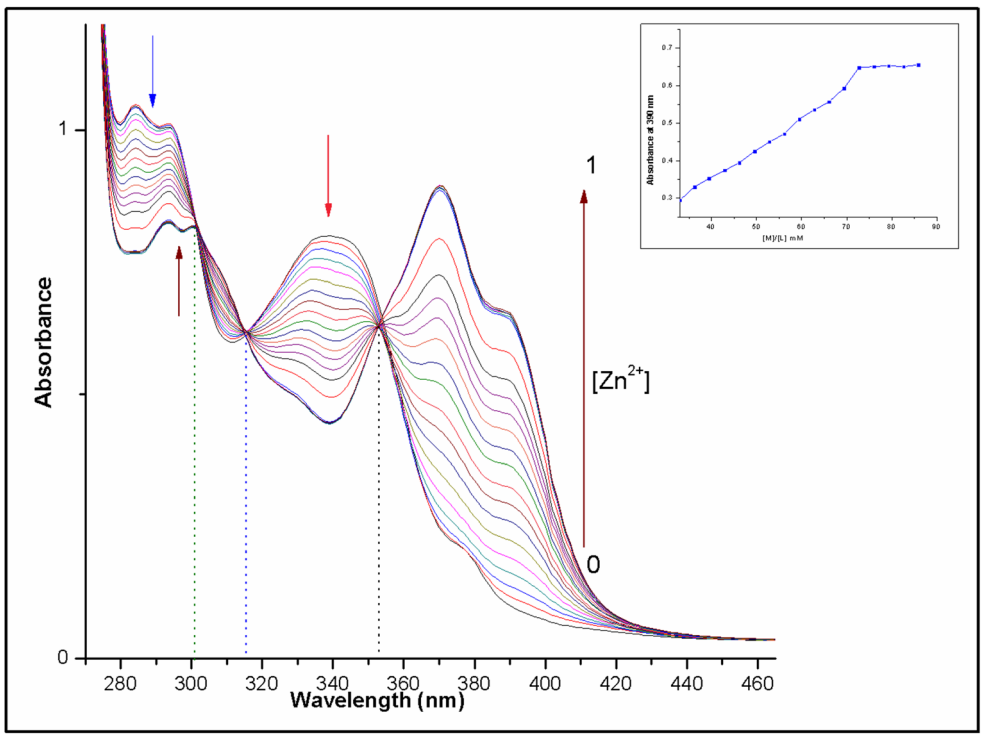

Fig. 4 UV–vis spectral changes of TBH (1×10^{-5} M) in the presence of different concentrations of Zn^{2+}ions in acetonitrile. Inset: UV–vis absorbance at 390 nm versus the number of equiv. of Zn^{2+} added

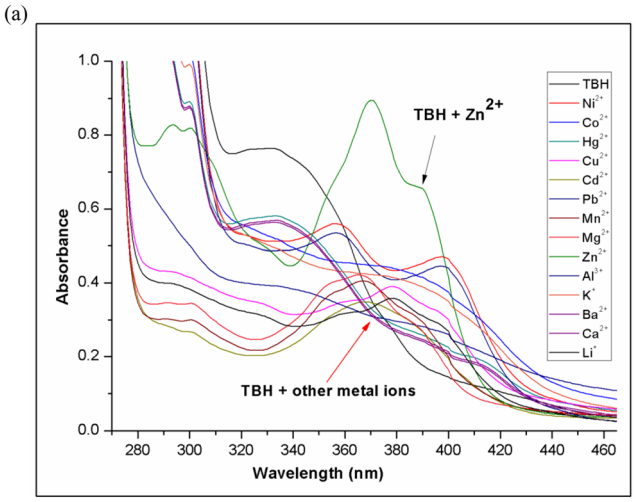

Fig. 5 **a** Absorbance spectral changes of TBH (1×10^{-5} M) in the presence of different metal nitrates (10 equiv.) such as Li^+, Na^+, K^+, Mg^{2+}, Ca^{2+}, Ba^{2+}, Mn^{2+}, Co^{2+}, Ni^{2+}, Cu^{2+}, Cd^{2+}, Hg^{2+}, Pb^{2+} and Al^{3+} at 390 nm in acetonitrile. **b** Bar graph shows the relative absorbance of TBH at 390 nm upon treatment with various metal ions

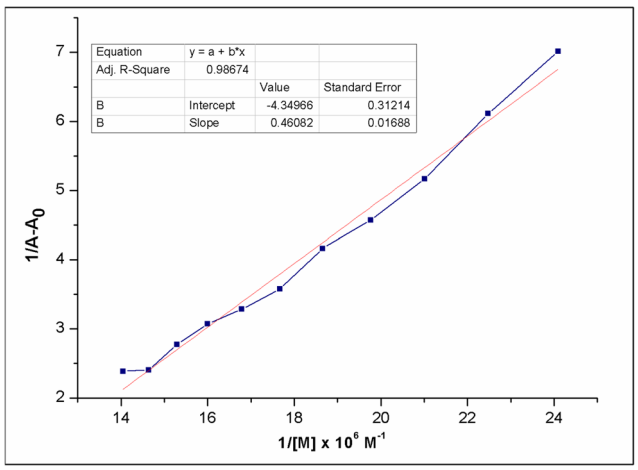

Fig. 6 Benesi-Hildebrand plot (absorbance at 390 nm) of TBH (1×10^{-5} M) based on UV- Vis titration, assuming 1:1 ratio for association between TBH and Zn^{2+}

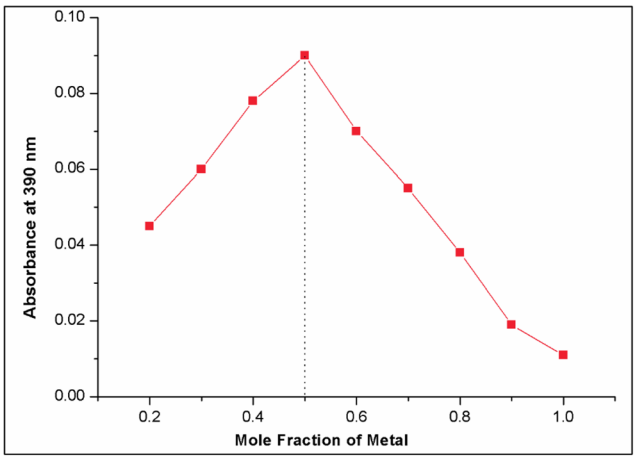

Fig. 7 Job plot for the binding of TBH with Zn^{2+} in acetonitrile. Absorbance at 390 nm was plotted as a function of the molar ratio $[Zn^{2+}]/([TBH] + [Zn^{2+}])$

Zn^{2+} Induced UV-Vis Spectroscopic Studies

The binding nature of **TBH** with Zn(II) ion was examined by performing the UV-Vis titration experiments. 3 mL of **TBH** (1×10^{-5} M in acetonitrile) is slowly titrated against hydrated Zn $(NO_3)_2$ (1×10^{-3} M, in acetonitrile) solution. An intense peak at 390 nm was noticed upon the addition of Zn (II) ion to **TBH**. The color of solution turns to pale fluorescent green, which signalize the formation of coordination complex (Fig. 4). Deprotonation results in increased binding ability of sensor **TBH** with Zn(II) ion [25]. When metal ions like Li^+, Na^+, K^+ (MNO_3), Ni^{2+}, Mn^{2+}, Ca^{2+}, Ba^{2+}, Mg^{2+}, Cu^{2+}, Co^{2+}, Hg^{2+}, Pb^{2+}, Cd^{2+}

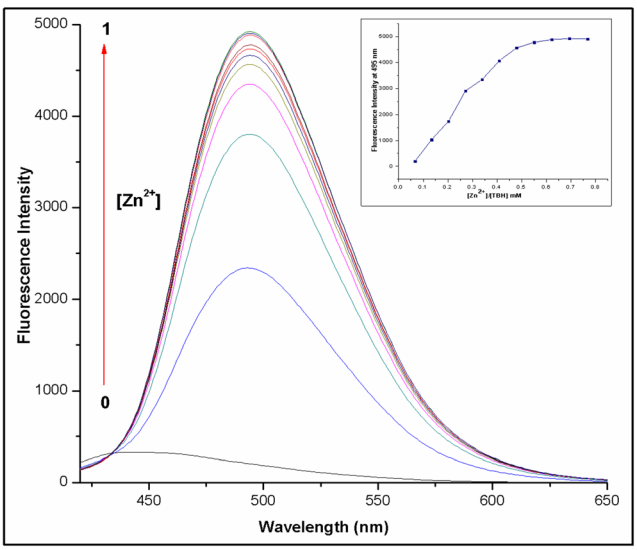

Fig. 8 Fluorescence spectral changes of TBH (1×10^{-5} M) in the presence of different concentrations of Zn^{2+} with an excitation at 390 nm in acetonitrile. Inset: Fluorescence intensity at 495 nm versus the number of equivalents of Zn^{2+} added

Scheme 2 The proposed mechanism of interaction between probe TBH and Zn^{2+}

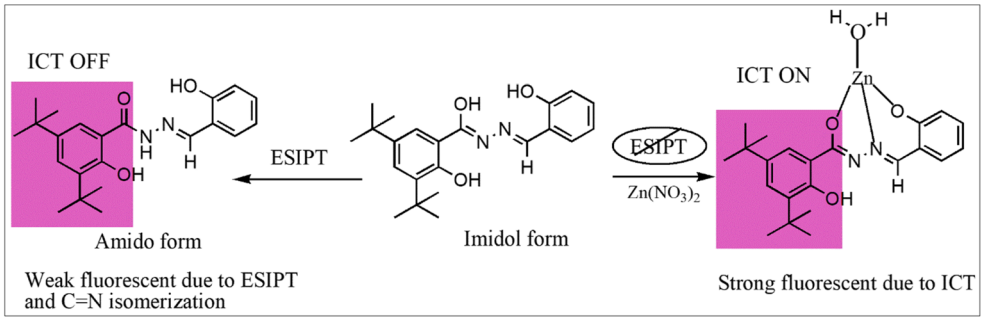

$(M(NO_3)_2)$ and Al^{3+} $(M(NO_3)_3)$ were added to solution of **TBH** in the presence and absence of the Zn(II) ion, no interference is observed indicating its high selectivity for Zn(II) ion (Fig. 5).

As shown in UV- Vis titration profile, with the increase in Zn(II) ion concentration from 0 to one equv. in TBH, results i) the decrease in the intensity of absorption bands at 284, 294 and 338 nm ii) the increase in the intensity of absorption band at 377 nm iii) the evolution of new peak at 390 nm due to intraligand charge transfer [ILCT] [26] and iv) the existence of the isosbestic points at 301, 315 and 353 indicating the formation of only one stable product which is in equilibrium with **TBH** at these wavelengths [27, 28]. The bands at 284 and 294 nm have suffered a slight red shift due to change in the planarity of sensor which opens the new door for greater electron delocalization when binds with Zn(II) ion [29]. Based on the UV- Vis titration data, association constant (K_a) was calculated using Benesi-Hildebrand equation and value comes as 2.17×10^9 M^{-1} (Fig. 6). The lowest detection limit was found to be 470×10^{-9} M (Fig. S9). The intersection of two lines at 0.5 mol fraction reveal that **TBH** and Zn(II) ion are in 1:1 stoichiometry (Fig. 7) [30, 31].

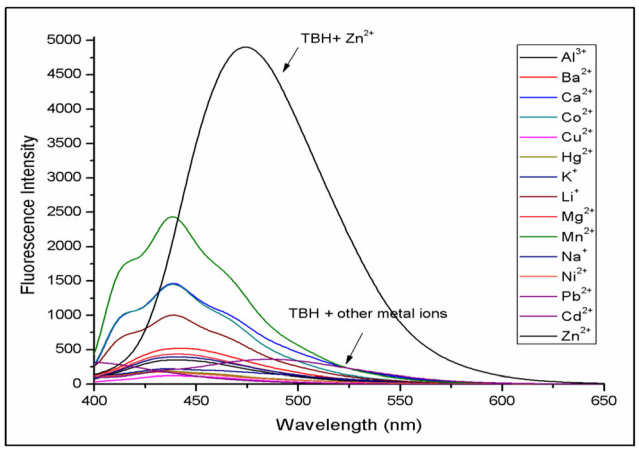

Fig. 9 Fluorescence spectral changes of TBH (1×10^{-5} M) in the presence of different metal nitrates (10 equiv.) such as Li^+, Na^+, K^+, Mg^{2+}, Ca^{2+}, Ba^{2+}, Mn^{2+}, Co^{2+}, Ni^{2+}, Cu^{2+}, Cd^{2+}, Hg^{2+}, Pb^{2+} and Al^{3+} with an excitation of 390 nm in acetonitrile

Zn^{2+} Induced Emission Spectroscopic Studies

The fluorescence spectra were recorded by titrating hydrated zinc nitrate (1×10^{-3} M) solution with 3 mL of **TBH** (1×10^{-5} M) solution in acetonitrile medium (Fig. 8). A bare sensor shows pale green fluorescence band at 443 nm (Φ =0.0178) when exited at 390 nm. Upon addition of Zn(II) ion to the sensor, a dark green fluorescence was observed at 495 nm (Φ =0.0319) which was more than 20-fold intense. An increase in the fluorescence intensity and red shift observed in **TBH** spectrum in presence of Zn^{2+} ion is due to blockage of ESIPT and -C=N isomerization process which increases the ICT character of **TBH** [29–33] during interaction (Scheme 2). The larger stoke shift (125 nm) further evidences the involvement of ESIPT process [34]. Other competing metal ions (20-fold excessive) such as K^+, Li^+, Na^+ (MNO_3), Mn^{2+}, Mg^{2+}, Ba^{2+}, Ca^{2+}, Cu^{2+}, Co^{2+}, Ni^{2+}, Hg^{2+}, Pb^{2+}, Cd^{2+} $(M(NO_3)_2)$ and Al^{3+} $(M(NO_3)_3)$

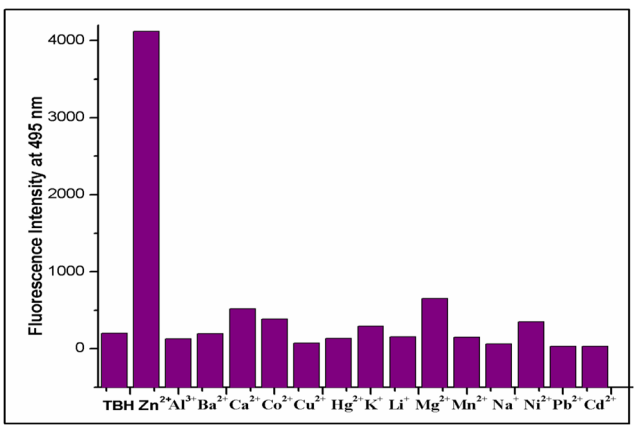

Fig. 10 Bar graph shows the relative emission intensity of TBH at 495 nm upon treatment with various metal ions

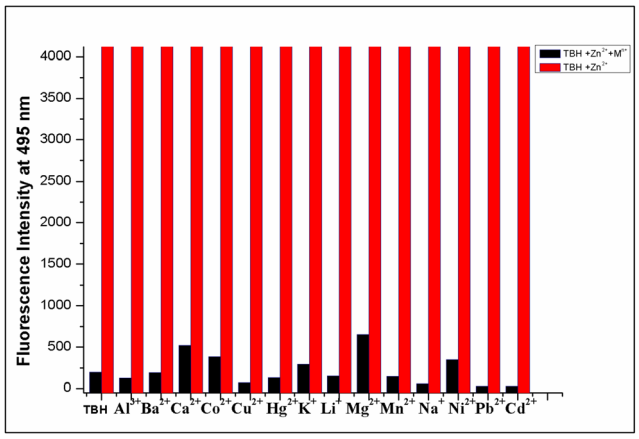

Fig. 11 Competitive experiment of TBH toward Zn^{2+} in the presence of other metal ions with an excitation of 390 nm in acetonitrile

didn't interrupt the spectral pattern of **TBH** in the presence and absence of zinc indicating its high specificity for zinc ion (Figs. 9, 10, and 11).

By using Banesi-Hildebrand equation (emission at 495 nm) the binding constant of **TBH**-Zn^{2+} complex was calculated and it comes as 3.77×10^4 M^{-1} (Fig. S12) [35]. Literature study reveals that, this value fits in the binding constants reported for Zn^{+2} ion in literature ($1.0–10^{12}$) [36, 37]. Limit of detection was calculated using ($3\sigma/K$) [38] and value obtained was 2.83×10^{-9} M (Fig. 12). This value is much lower than World Health Organization (WHO) guideline (76 μM) in drinking water [39]. Job's plot experimental results reflects that **TBH** and Zn(II) ion are in 1:1 stoichiometry (Fig. S11) [30, 31].

pH Dependent Studies

The effect of pH on the photophysical properties of **TBH** and its zinc complex was studied in Phosphate buffered saline (PBS) to apply to the environmental and biological systems [40–42]. The effect of pH on optical properties of **TBH** shows that, at lower pH range (3–6), no significant changes were observed. In the range of pH 7–8, the receptor has shown a very high absorbance and strong fluorescence, which may be due to deprotonation of -OH groups, followed by its coordination to metal ion. As the pH increased beyond 8, the absorbance and fluorescence intensity has gradually decreased, which may be due to the formation of Zn $(OH)_2$ or Zn $(OH)^{2+}$ [Fig. S10 & 13] [27, 28]. The pH studies clearly suggest that, receptor could render pH dependent fluorescence measurements in a live physiological environment. The sensing capability for Zn(II) ion under physiological conditions, and also its high detection capability even at low concentrations are the advantages of the present molecule.

NMR Titration Experiment and ESI-Mass Studies

In order to understand the binding mode of **TBH** with Zn(II) ion and also to study the structural changes in the **TBH** on formation of complex, we took ^{1}H-NMR titration studies in DMSO–d_6 (Fig. 14). A very significant changes were observed during NMR titration, mainly with the signal for -O1H, -O3H, C7H and -N2H. These signals are very much intense in free **TBH** and were observed at 12.15, 12.99, 8.78 and 11.08 ppm respectively. The reduction in the intensity of hydroxyl group –O1H and also for -N2H was observed when 0.5 equivalent of hydrated $Zn(NO_3)_2$ solution was added and these two signals have completely disappeared when one equivalent of hydrated $Zn(NO_3)_2$ solution was added. This indicates that, **TBH** is coordinated to the metal ion through *ONO* donor set of atoms via deprotonation of O1H and N2H (Scheme 1). The signal due

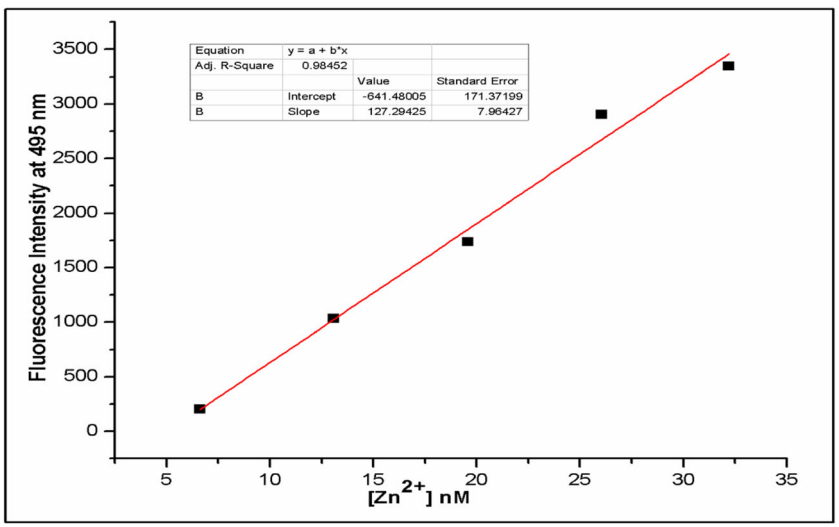

Fig. 12 Limit of detection based on change in the ratio (fluorescence intensity at 495 nm) of TBH with Zn^{2+}

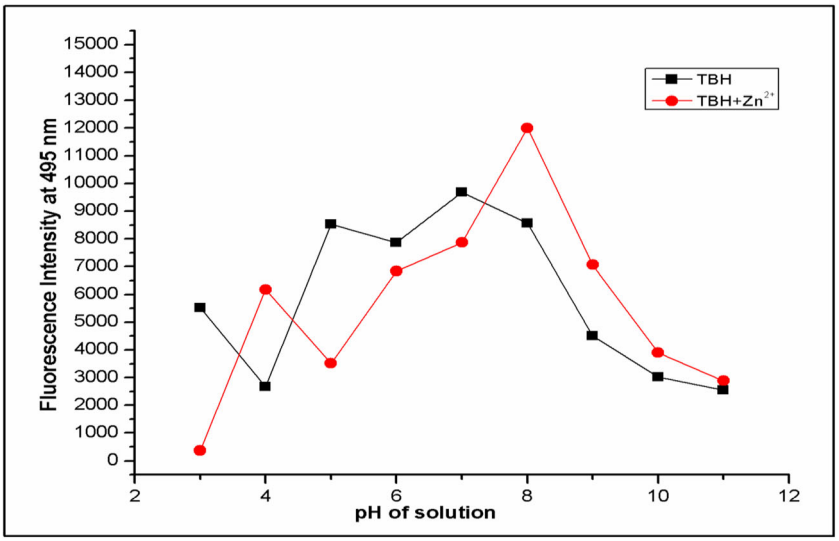

Fig. 13 Fluorescence intensities of TBH (1×10^{-5} M) and of TBH-Zn^{2+} complex, respectively, at different pH values (3–11) in PBS Buffer solution

to O3H has shifted to 14.17 ppm due to involvement in hydrogen bonding and that of C7H has shifted to 8.57 ppm upon coordination with Zn(II) ion due to change in electron density around it. To further support the binding nature, ESI mass spectroscopic analysis was carried out. Upon the addition of one equivalent of Zn(II) ion, positive mode ESI-mass spectrum of **TBH** shows the peak at 451 m/z, which corresponds to the formation **TBH**-Zn^{2+} complex with 1:1 stoichiometry (Fig. S7).

Solvent Effect

We examined optical properties of **TBH** in various solvents like Dimethylformamide, Acetone, Dimethyl

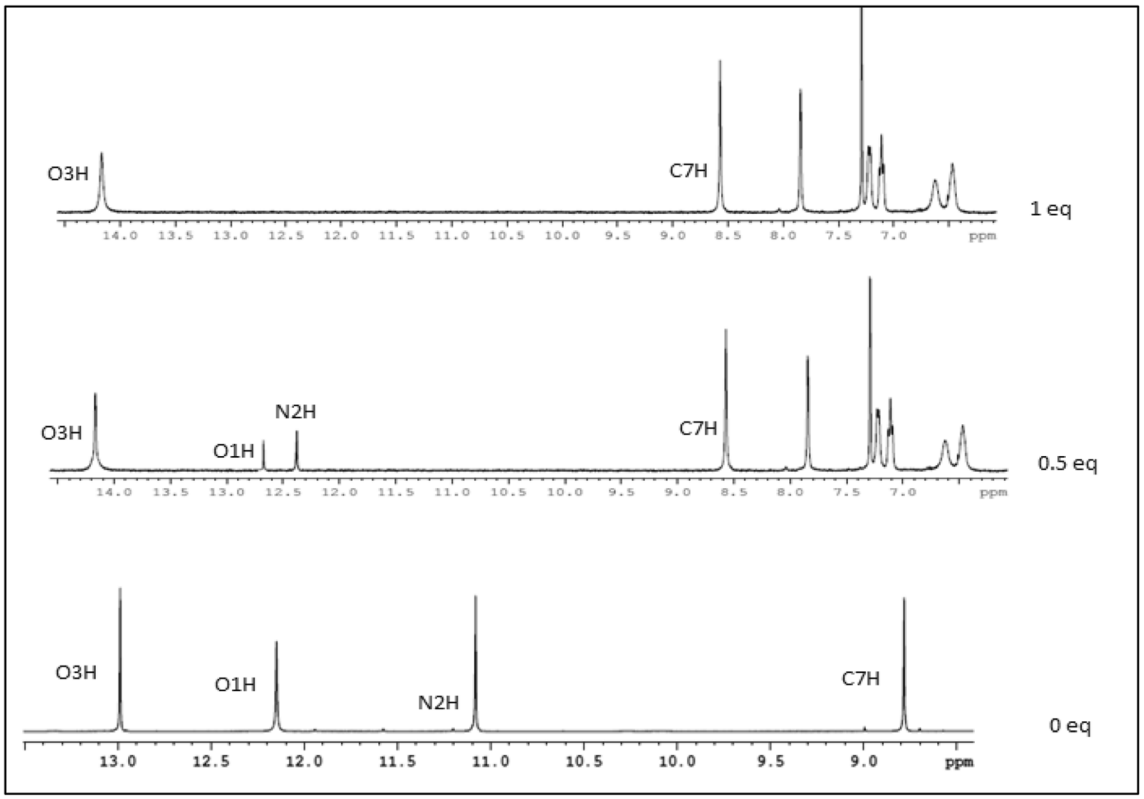

Fig. 14 ^{1}H NMR titration of TBH with hydrated Zn $(NO_3)_2$

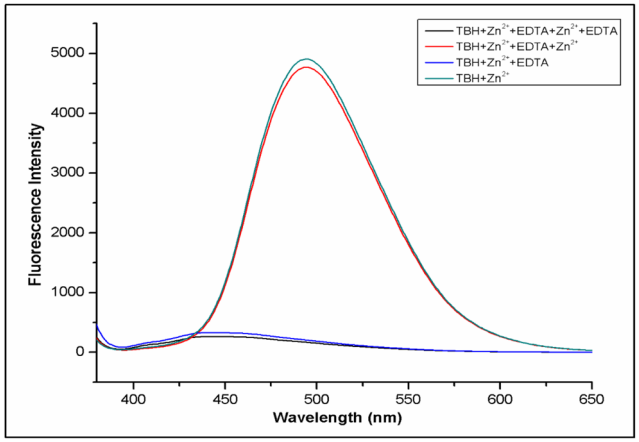

Fig. 15 Fluorescence spectra showing reversibility of Zn^{2+} coordination to TBH by EDTA

sulfoxide, Ethyl acetate, Chloroform, Benzene, Ethanol, Methanol and Tetrahydrofuran (Fig. S13). Electronic system of **TBH** was disturbed by the polarity/strong hydrogen bonding character of the solvent. The interaction of polar solvents with **TBH** stabilizes and reduces the energy barrier between HOMO-LUMO and thus emit high fluorescence [43]. To support this, quantum yield calculations were carried out in two polar solvents (Table 1). The results indicate that, with increase in polarity of the solvent, quantum yield is also increasing. Ethyl acetate, Ethanol and Dimethyl sulfoxide showed good fluorescence emission, whereas, low fluorescence intensity was observed in other solvents.

Reversibility of TBH

Reversibility of **TBH** by the alternative addition of Na_2EDTA for **TBH**-Zn(II) ion in acetonitrile was carried out [44, 45]. Quenching in the fluorescence intensity of **TBH**-Zn^{2+} complex was observed at 495 nm upon addition of EDTA, whereas, an enhancement was observed at 443 nm. The fluorescence intensity at 495 nm is revived again on addition of Zn(II) ion, showing reversible behavior of **TBH** for Zn(II) ion. Strong affinity of EDTA for the Zn(II) ion causes decrease in the florescence intensity by forming EDTA-Zn^{2+} complex and sensor **TBH** is regenerated (Fig. 15). Therefore, the **TBH** could act as a selective fluorescent sensor for recognition of Zn(II) ion.

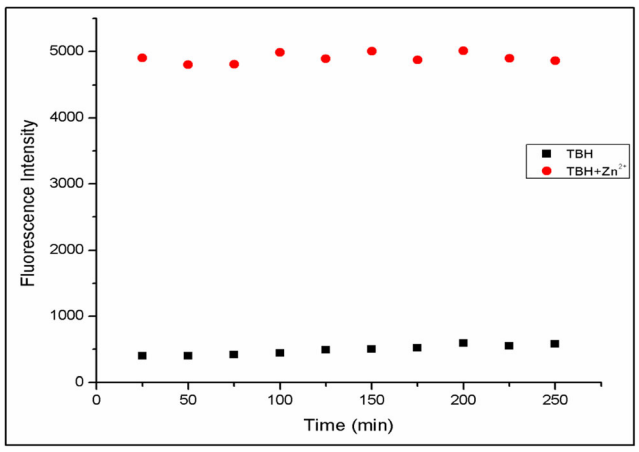

Fig. 16 Photostabilities of TBH and of TBH -Zn^{2+} complex

Effect of Reaction Time and Photostability

An bare sensor shows weak fluorescence intensity at 493 nm exhibiting high stability at room temperature. Upon addition of one equv. of Zn(II) ion, fluorescence intensity of **TBH** increases suddenly showing its high reactivity for Zn(II) ion and attains maximum within 8 min indicating the completion of reation and remains constant for few minutes reflecting its stability under room temperature (Fig. 16 & S14).

TD-DFT Calculation and Sensing Mechanism

The experimental studies of Jobs plot, ^{1}H-NMR titrations and ESI-Mass analysis suggest the 1:1 stoichiometry of **TBH** to Zn(II) ion. In order to deepen our knowledge into fluorescent sensing mechanism of **TBH** towards Zn(II) ion, theoretical studies were also carried out. The energy minimized structures of **TBH** and **TBH**-Zn^{2+}complex (Fig. 17) were optimized in acetonitrile by applying Density Functional Theory (DFT/B3LYP). The HOMO of **TBH** is localized on the salicylaldehyde benzene ring along with coordinating atoms while in the LUMO it is extended to tertiary-butyl group substituted benzene ring. On the contrary, both HOMO and LUMO of **TBH**-Zn^{2+} complex were localized on both benzene rings in addition to coordinating atoms.

In theoretically calculated absorption spectrum, **TBH** exhibit intramolecular charge transfer (ICT) band located at λ_{Theo} 341 nm ($\lambda exp = 335$ nm) which shift to λ_{Theo} 394 nm ($\lambda exp = 390$ nm) upon complexation with Zn(II) ion. Free **TBH** exhibit a characteristic sharp band at 294 nm (λ_{Theo} 304 nm) due to $n \rightarrow p^*$ of -HC=N- group. Upon complexation with the Zn(II) ion, this band was red shifted to 337 nm (λ_{Theo} 330 nm). The experimental observed results were well supported by theoretical results (Table 2 & Fig. S16). Furthermore, the energy gap (ΔE) between the HOMO-LUMO of the receptor **TBH** and **TBH**-Zn^{2+} complex is examined (Fig. 18).

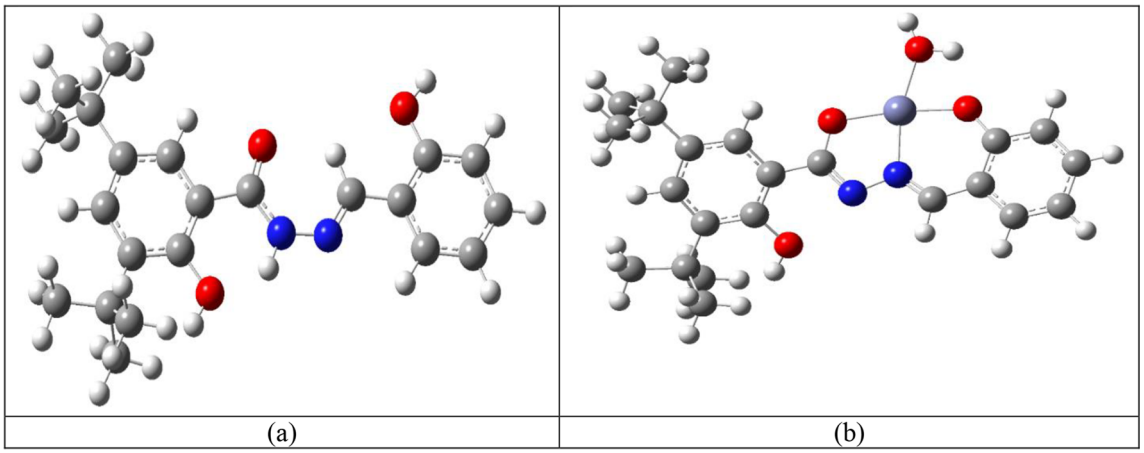

Fig. 17 The energy-minimized structures of (**a**) TBH and (**b**) TBH -Zn^{2+} complex

Compared to the free TBH (ΔE = 4.20 eV), the energy gap in presence of the Zn(II) ion is less (ΔE = 3.64 eV), which are in consistant with the experimentally observed results [46–48].

Cytotoxicity Test for TBH

MTT assay method was employed to determine the cytotoxicity of **TBH** against HeLa cells. The viability of HeLa cells was studied by treating with **TBH** over a range of concentrations (12.5, 25, 50,100 and 200 μM) for 24 h [44, 45]. At 12.5 μM, the cells viability was over 98.07% of control, whereas at 200 μM it was 64.09% (Fig. S15). These results indicate that at lower concentrations, **TBH** produced no cytotoxicity in HeLa cells, which means it may be useful as a sensor to detect Zn(II) ion in biological systems.

Fluorescence Imaging in HeLa Cells

The fluorescence response of **TBH** towards Zn(II) ion in HeLa cells was studied to check its practical application using bio-imaging experiment (Fig. 19). The HeLa cells were incubated with 10 μM **TBH** for 30 min at 37 °C.

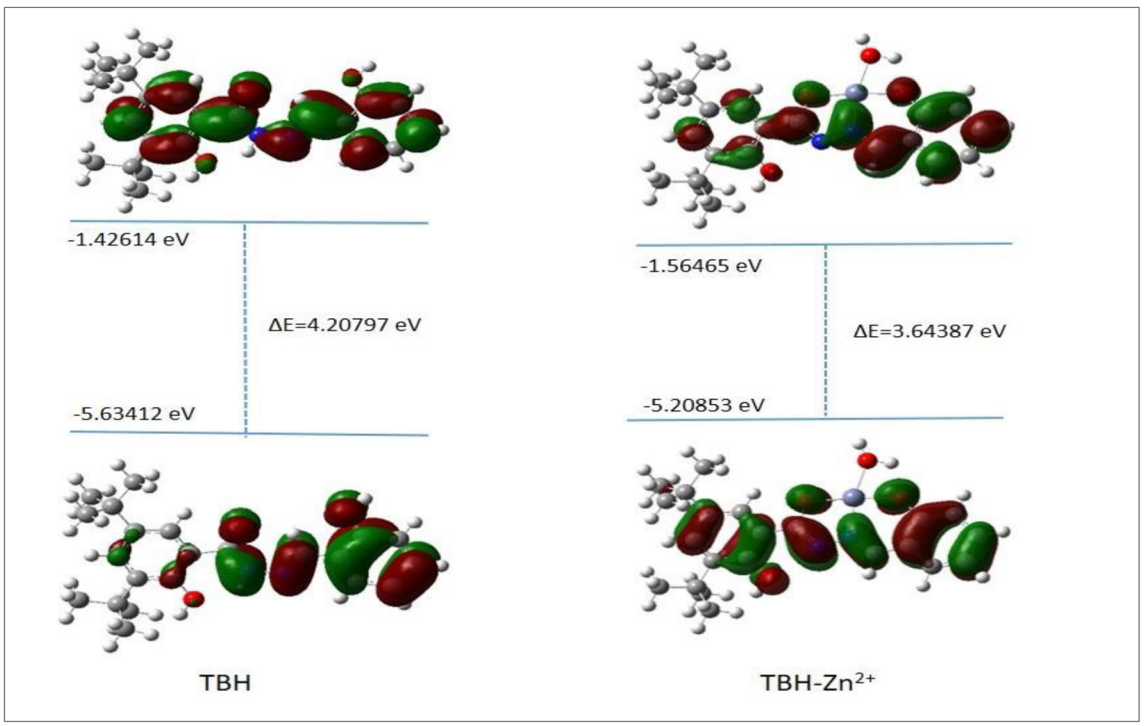

Fig. 18 Molecular orbital geometry and the HOMO – LUMO energy gap of TBH and of TBH -Zn^{2+} complex

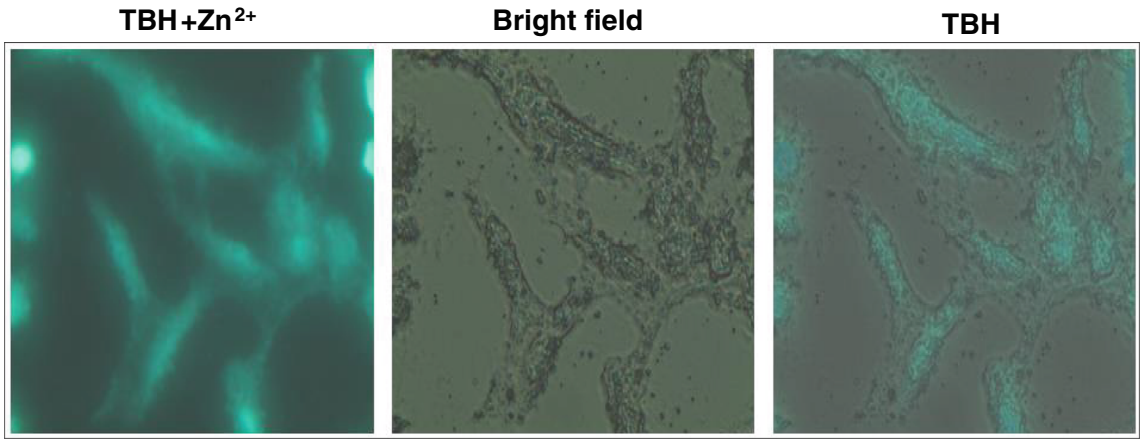

Fig. 19 Fluorescent imaging of HeLa cells incubated with TBH followed by the addition of Zn^{2+}.The cells were treated with TBH (10 μM) for 30 min, washed with PBS, and incubated with 10 μM of Zn^{2+}. λex = 390 nm, λem = 495 nm

The light green fluorescence emitted by **TBH** in the resulting confocal fluorescent images indicate that, it can penetrates into the HeLa cells and has excellent staining property. To determine the response of **TBH** to intracellular Zn(II) ion, 10 μM Zn(II) ion was incubated to preloaded HeLa cells for 30 min at 37 °C and resultant images were captured [49–51]. It is noticed that, **TBH** alone exhibits weak fluorescence but in presence of Zn(II) ion, it exhibit a strong turn on green fluorescence suggesting it could penetrate living cells and subsequently respond to intracellular Zn(II) ion.

Conclusion

We have developed a novel switch on optical probe (**TBH**), which selectively interact with Zn(II) ion in CH_3CN medium. **TBH** shows fast response towards Zn(II) ion in 1:1 stoichiometric manner, which induce a color change from colorless to yellow by increasing fluorescence intensity selectively for Zn(II) ion over other cations. The detection limits of **TBH** for Zn(II) ion reaches to nanomolar level. The DFT calculations explore the sensing mechanism of **TBH** for Zn(II) ion. The host molecule could be recyclable simply by treating with a proper reagent such as Na_2EDTA. Moreover, **TBH** could also be used for intracellular Zn (II) ion imaging by confocal fluorescence microscopy for further application. Finally, we believe that **TBH** could serve as a promising molecular sensor for the determination of Zn(II) ion in chemical, biological and environmental systems and contribute to the development of novel optical probes.

Acknowledgements The authors thank USIC, Karnatak University, Dharwad for electronic spectral analyses and Indian Institute of Science, Bangalore for recording NMR spectra. Two of the authors (M. B. B and G. H. C.) are grateful to UGC for awarding a RFSMS fellowship.

References

1. Vigato PA, Peruzzo V, Tamburini S (2012) Acyclic and cyclic compartmental ligands: Recent results and perspectives. Coord Chem Rev 256:953–1114
2. Wang X, Liu Z, Qian F, He W (2012) A bezoimidazole-based highly selective and low-background fluorescent sensor for Zn2+. Inorg Chem Commun 15:176–179
3. Basoglu A, Parlayan S, Ocak M, Alp H, Kantekin H, Ozdemir M, Ocak U (2009) Selective Recognition of Cobalt (II) Ion by a New Cryptand Compound with N2O2S2 Donor Atom Possessing 2-Hydroxy-1-Naphthylidene Schiff Base Moiety. J Fluoresc 19: 655–662
4. Jeong Y, Yoon J (2012) Recent progress on fluorescent chemosensors for metal ions. Inorg Chim Acta 381:2–14
5. Zhang JF, Zhou Y, Yoon J, Kim JS (2011) Recent progress in fluorescent and colorimetric chemosensors for detection of precious metal ions (silver, gold and platinum ions). Chem Soc Rev 40:3416
6. Cheng J, Ma X, Zhang Y, Liu J, Zhou X, Xiang H (2014) Optical Chemosensors Based on Transmetalation of Salen-Based Schiff Base Complexes. Inorg Chem 53:3210–3219
7. Yang Z, Yan C, Chen Y, Zhu C, Zhang C, Dong X, Yang W, Guo Z, Lu Y, He W (2011) A novel terpyridine/benzofurazan hybrid fluorophore: metal sensing behavior and application. Dalton Trans 40:2173–2176
8. Vongnam K, Aree T, Sukwattanasinitt M, Rashatasakhon P (2018) ChemistrySelect 3:3495
9. Alam R, Mistri T, Bhowmick R, Katarkar A, Chaudhuri K, Ali M (2016) ESIPT blocked CHEF based differential dual sensor for Zn2+and Al3+in a pseudo-aqueous medium with intracellular bio-imaging applications and computational studies. RSC Adv 6: 1268–1278
10. Bothra S, Paira P, Ashok Kumar SK, Kumar R, Sahoo SK (2017) Vitamin B6 Cofactor-Conjugated Polyethyleneimine-Passivated Silver Nanoclusters for Fluorescent Sensing of Zn2+ and Cd2+ Using Chemically Modified Cellulose Strips. ChemistrySelect 2: 6023–6029
11. Ali H, Khan E (2017) Bioaccumulation of non-essential hazardous heavy metals and metalloids in freshwater fish. Risk to human health. Environ Chem Lett 15:329–917. https://doi.org/10.1007/s10311-018-0734-7
12. Lin L, Wang D, Chen SH, Wang DJ, Yin GD (2017) A highly sensitive fluorescent chemosensor for selective detection of zinc (II) ion based on the oxadiazole derivative. Spectrochim Acta A Mol Biomol Spectrosc 174:272–278

13. Naik K, Revankar V (2018) Bis-(2-Hydroxybenzylidene)-1H-Pyrazole 3,5-Dicarbohydrazide as a Novel Chemosensor for the Detection of Endogenous Zinc: A Fluorometric Study. J Fluoresc 28:1105–1114. https://doi.org/10.1007/s10895-018-2273-9
14. Kim YS, Lee JJ, Lee SY, Kim PG, Kim C (2016) A Turn-on Fluorescent Chemosensor for Zn2+ Based on Quinoline in Aqueous Media. J Fluoresc 26:835–844
15. Patila M, Keshav K, Kumawat MK, Bothrad S, Sahood SK, Srivastava R, Rajputa J, Bendrea R, Kuwara A (2018) Monoterpenoid derivative based ratiometric fluorescent chemosensor for bioimaging and intracellular detection of Zn2+ and Mg2+ ions. J Photochem Photobiol A Chem 364:758–763
16. Becker JS, Zoriy M, Pickhardt C, Przybylski M, Becker JS (2005) Investigation of Cu-, Zn- and Fe-containing human brain proteins using isotopic-enriched tracers by LA-ICP-MS and MALDI-FT-ICR-MS. Int J Mass Spectrom 242:135–144
17. Chen J, Teo KC (2001) Determination of cadmium, copper, lead and zinc in water samples by flame atomic absorption spectrometry after cloud point extraction. Anal Chim Acta 450:215–222
18. Binet MRB, Ma R, McLeod CW, Poole RK (2003) Detection and characterization of zinc- and cadmium-binding proteins in Escherichia coli by gel electrophoresis and laser ablation-inductively coupled plasma-mass spectrometry. Anal Biochem 318:30–38
19. Li Z, Yang G, Wang B, Jiang C, Yin J (2002) Determination of transition metal ions in tobacco as their 2-(2-quinolinylazo)-5-dimethylaminophenol derivatives using reversed-phase liquid chromatography with UV–VIS detection. J Chromatogr A 971:243–248
20. Li GY, Han KL (2018) Advanced review, vol 8, p 2
21. Chimmalagi GH, Kendur U, Patil SM, Gudasi KB, Frampton CS, Budri MB, Mangannavar Cr V, Muchchandi IS (2018) Appl Organomet Chem 32:4337
22. Budri M, Kadolkar P, Gudasi K, Inamdar S (2019) A highly selective and sensitive turn on optical probe as a promising molecular platform for rapid detection of Zn (II) ion in acetonitrile medium: Experimental and theoretical investigations. J Mol Liq 283:346–358. https://doi.org/10.1016/j.molliq.2019.03.097
23. G. W. Trucks, H. B. Schlegel, G. E. Scuseria, M. A. Robb, J. R. Cheeseman, G. Scalmani, V. Barone, B. Mennucci, G. A. Petersson, H. Nakatsuji, M. Caricato, X. Li, H. P. Hratchian, A. F. Izmaylov, J. Bloino, G. Zheng, J. L. Sonnenberg, M. Hada, M. Ehara, K. Toyota, R. Fukuda, J. Hasegawa, M. Ishida, T. Nakajima, Y. Honda, O. Kitao, H. Nakai, T. Vreven, J. A. Montgomery, Jr., J. E. Peralta, F. Ogliaro, M. Bearpark, J. J. Heyd, E. Brothers, K. N. Kudin, V. N. Staroverov, T. Keith, R. Kobayashi, J. Normand, K. Raghavachari, A. Rendell, J. C. Burant, S. S. Iyengar, J. Tomasi, M. Cossi, N. Rega, J. M. Millam, M. Klene, J. E. Knox, J. B. Cross, V. Bakken, C. Adamo, J. Jaramillo, R. Gomperts, R. E. Stratmann, O. Yazyev, A. J. Austin, R. Cammi, C. Pomelli, J. W. Ochterski, R. L. Martin, K. Morokuma, V. G. Zakrzewski, G. A. Voth, P. Salvador, J. J. Dannenberg, S. Dapprich, A. D. Daniels, O. Farkas, J. B. Foresman, J. V. Ortiz, J. Cioslowski, and D. J. Fox, (2013) Gaussian, Inc., Gaussian 09, Revision, D.01, M. J. Frisch, Wallingford CT
24. Patil SM, Vadavi RS, Kendur U, Pujar GH, Chimmalagi G, Kulkarni SD, Nethaji M, Nembenna S, Inamdar SR, Gudasi KB (2017) Jrnl Photochemistry and Photobiology A: Chemistry 351:225
25. Yu F, Guo X, Tian X, Jia L (2017) A Ratiomeric Fluorescent Sensor for Zn2+ Based on N,N′-Di(quinolin-8-yl)oxalamide. J Fluoresc 27:723–728
26. Budri M, Kadolkar P, Gudasi K, Inamdar S (2019) Jrnl Mol Liq. https://doi.org/10.1016/j.molliq.2019.03.097
27. Roy N, Dutta A, Mondal P, Paul PC, Sanjoy Singh T (2017) Coumarin Based Fluorescent Probe for Colorimetric Detection of Fe3+ and Fluorescence Turn On-Off Response of Zn2+ and Cu2+. J Fluoresc 27:1307–1321
28. Bothra S, Babu LT, Paira P, Ashok Kumar SK, Kumar R, Sahoo SK (2018) A biomimetic approach to conjugate vitamin B6 cofactor with the lysozyme cocooned fluorescent AuNCs and its application in turn-on sensing of zinc(II) in environmental and biological samples. Anal Bioanal Chem 410(1):201–210
29. Kumar V, Diwan U, Sanskriti I, Mishra RK, Upadhyay KK (2017) ChemistrySelect 2:11358
30. Qin J, Li T, Wang B, Yang Z, Fan L (2014) Fluorescent sensor for selective detection of Al3+ based on quinoline–coumarin conjugate. SPECTROCHIM ACTA A 133:38–43
31. Anand T, Kumar SKA, Sahoo SK (2017) ChemistrySelect 2(25):7570
32. Wu J, Liu W, Ge J, Zhang H, Wang P (2011) Chem Soc Rev 40:33
33. Udhayakumari D, Saravanamoorthy S, Ashok M, Velmathi S (2011) Simple imine linked colorimetric and fluorescent receptor for sensing Zn2+ ions in aqueous medium based on inhibition of ESIPT mechanism. Tetrahedron Lett 52:4631–4635
34. Boonkitpatarakul K, Smata A, Kongnukool K, Srisurichanb S, Chainokc K, Sukwattanasinitt M (2018) An 8-aminoquinoline derivative as a molecular platform for fluorescent sensors for Zn(II) and Cd(II) ions. J LUMIN 198:59–67
35. Choi JY, Kim D, Yoon J (2013) A highly selective "turn-on" fluorescent chemosensor based on hydroxy pyrene–hydrazone derivative for Zn2+. Dyes Pigments 96:176–179
36. Lin AWH, Cheng P, Wan C, Wu A (2012) A turn-on and reversible fluorescence sensor for zinc ion. Analyst 137:4415
37. Lohani CR, Kim J, Chung S, Yoon J, Lee K (2010) Colorimetric and fluorescent sensing of pyrophosphate in 100% aqueous solution by a system comprised of rhodamine B compound and Al3+ complex. Analyst 135:2079
38. Park GJ, Lee JJ, You GR, Nguyen L, Noh I, Kim C (2016) A dual chemosensor for Zn 2+ and Co 2+ in aqueous media and living cells: Experimental and theoretical studies. Sensors Actuators B Chem 223:509–519
39. Balamurugan G, Velmathi S (2017) Sensors Actuators B 23386:8
40. Christian GD, Purdy WC (1962) The residual current in orthophosphate medium. J Electroanal Chem 3:363–367
41. Goyal RN, Gupta VK, Chatterjee S (2009) Fullerene-C60-modified edge plane pyrolytic graphite electrode for the determination of dexamethasone in pharmaceutical formulations and human biological fluids. Biosens Bioelectron 24:1649–1654
42. Goyal RN, Guptaa VK, Chatterjeea S (2010) Electrochemical investigations of corticosteroid isomers—testosterone and epitestosterone and their simultaneous determination in human urine. Anal Chim Acta 657:147–153
43. Tabakci SEB (2017) Jrnl. Fluoresc 27:2145
44. Shah T, Joshi K, Mishra S, Otiv S, Kumbar V (2016) Molecular and cellular effects of vitamin B12 forms on human trophoblast cells in presence of excessive folate. Biomed Pharmacother 84:526–534
45. Tayade K, Bondhopadhyay B, Keshav K, Sahoo SK, Basu A, Singh J, Singh N, Nehete DT, Kuwar A (2016) A novel zinc(ii) and hydrogen sulphate selective fluorescent "turn-on" chemosensor based on isonicotiamide: INHIBIT type's logic gate and application in cancer cell imaging. Analyst 141(5):1814–1821
46. Anitha C, Sheela CD, Tharmaraj P, Shanmugakala R (2012) Studies on Synthesis and Spectral Characterization of Some Transition Metal Complexes of Azo-Azomethine Derivative of Diaminomaleonitrile. Int J Inorg Chem 2013:1–10. https://doi.org/10.1155/2013/436275
47. Said MH (2016) Int J Chemtech Res 9:111
48. Temel H, Ilhan S (2009) Synthesis and spectroscopic studies of novel transition metal complexes with schiff base synthesized from

1,4-bis-(o-aminophenoxy)butane and salicyldehyde. Russ. J Inorg Chem 54:543–547
49. Bhat SS, Revankar VK, Kumbar V, Bhat K, Vitthal A (2018) Kawade. Acta Cryst C74:146
50. Patil M, Bothra S, Sahoo SK, Rather HA, Vasita R, Bendre R, Kuwar A (2018) Highly selective nicotinohydrazide based 'turn-on' chemosensor for the detection of bioactive zinc(II): Its biocompitability and bioimaging application in cancer cells. Sensors Actuators B 270:200–206
51. Upadhyayaa Y, Ananda T, Babub LT, Pairab P, Crisponic G, Ashok Kumar SK, Kumara R, Sahooa SK (2018) Three-in-one type fluorescent sensor based on a pyrene pyridoxal cascade for the selective detection of Zn(ii), hydrogen phosphate and cysteine. Dalton Trans 47(3):742–749